Article

Upgrading Bio-oil Quality via Pressurized Air Pretreatment of Lignocellulosic Biomass

Janewit Wannapeera [1,2], Thipsuphin Hinsui [2], Supachai Jadsadajerm [3], Pansa Liplap [1,2,*]

[1] School of Agricultural Engineering, Institute of Engineering, Suranaree University of Technology, Nakhon Ratchasima 30000, Thailand; janewit@sut.ac.th (JW)

[2] Center of Excellence in Biomass, Suranaree University of Technology, Nakhon Ratchasima 30000, Thailand; hinsui.t@g.sut.ac.th (TH)

[3] Department of Industrial Chemistry, Faculty of Applied Science, King Mongkut's University of Technology North Bangkok, Bangkok 10800, Thailand; supachai.j@sci.kmutnb.ac.th (SJ)

* Correspondence: Pansa Liplap, E-mail: pansa@g.sut.ac.th

ABSTRACT

This study investigates the application of low-temperature pressurized air oxidation as a pretreatment method to enhance the chemical quality of bio-oil derived from lignocellulosic biomass. Rice straw (RS) and eucalyptus wood (EUCA) were subjected to oxidation pretreatment at 250 °C under various pressures (0.1–1.0 MPa) before pyrolysis at 550 °C. The results show that pretreatment under moderate pressures (0.5–1.0 MPa) significantly influenced the chemical composition of the resulting bio-oil. Gas chromatography-mass spectrometry (GC-MS) analysis revealed a reduction in oxygenated compounds, such as alcohols and ketones, and an increase in long-chain aliphatic hydrocarbons such as dodecane and pentadecane. These compositional changes reflect the potential for improved chemical stability and deoxygenation, which are beneficial for downstream fuel upgrading. Although the bio-oil yield decreased with increasing pretreatment severity, the enhancement in chemical quality supports the application of pressurized air oxidation as an effective method for producing upgraded bio-oil from lignocellulosic feedstocks.

KEYWORDS: pressurized air oxidation; pressurized air pretreatment; low temperature treatment; bio-oil upgrading; pyrolysis

Received: 6 Jul 2025
Accepted: 20 Oct 2025
Published: 24 Oct 2025

INTRODUCTION

The rising global energy demand and environmental concerns, including climate change and air pollution, have intensified the search for renewable and sustainable energy alternatives. Biomass, as a carbon-neutral and abundantly available resource, plays a pivotal role in the transition toward a bio-based economy. Among thermochemical

conversion technologies, the pyrolysis of lignocellulosic biomass into bio-oil presents a promising route for producing liquid fuels and value-added chemicals [1–3].

In Thailand, the utilization of agricultural residues and other biomass waste streams aligns with strategic national agendas such as the Bio-Circular-Green (BCG) Economy Model and the Bioeconomy Development Plan. These frameworks, part of the “New S-Curve” industrial strategy introduced in 2016, aim to enhance sustainability and economic resilience by transforming low-value biomass into high-value bio-based products and fuels [4,5]. Within this context, the development of advanced biomass conversion technologies is critical to optimizing resource efficiency and reducing dependence on imported fossil fuels.

Bio-oil, the primary liquid product of pyrolysis, comprises a complex mixture of oxygenated organic compounds, including acids, aldehydes, ketones, and phenolics [6]. While it offers potential as a heating fuel and as a feedstock for chemicals, raw bio-oil suffers from several drawbacks, such as high oxygen and water content, low heating value, chemical instability, and corrosiveness. These limitations hinder its direct utilization and long-term storage, necessitating further upgrading to enhance its physicochemical properties and fuel quality [7–9].

Various strategies have been explored to improve bio-oil quality, including catalytic pyrolysis, vapor-phase upgrading, and feedstock pretreatment. Among them, pretreatment of biomass prior to pyrolysis is considered an effective and scalable approach that alters the structure and composition of feedstock, thereby influencing both the yield and quality of bio-oil [10–13]. Torrefaction, a mild thermal pretreatment conducted under inert conditions, has been extensively investigated to enhance the properties of biomass, including energy density, hydrophobicity, and grindability. However, conventional torrefaction often suffers from tar condensation and system fouling, particularly at elevated temperatures (>300 °C) and when recycling flue gases [14–16]. Oxidative torrefaction, employing air or flue gas as the reaction medium, has also been explored as an alternative pretreatment. However, the solid yields are generally lower than those from classical torrefaction due to partial oxidative combustion. In terms of fuel quality, improvements such as reduced O/C and H/C ratios and enhanced hydrophobicity have been reported, but the outcomes are often more variable and sometimes less favorable than those obtained under inert conditions, reflecting the susceptibility of the process to over-oxidation [17–22]. Pressurized torrefaction has shown potential to overcome these drawbacks and improve solid fuel characteristics, although it typically requires high pressures (>4 MPa) and inert environments, which increase system complexity and capital costs [23–27].

To address these limitations, a new pretreatment technique known as pressurized air oxidation has recently been proposed. Studies exploring pressurized oxidative conditions remain scarce; to our knowledge, the highest pressure previously reported was approximately 600 kPa [22]. It

has been demonstrated in previous studies that higher pressures can further enhance carbon enrichment and improve the thermal stability of the solid fraction [23]. Building on this concept, the present work extends pressurized air oxidation to pressures up to 1.0 MPa under relatively low temperatures (<250 °C), aiming to evaluate not only the upgraded solid but also, its influence on bio-oil yield and chemical composition. Nevertheless, current studies remain limited, with most of the existing literature focusing primarily on the solid fraction. To our knowledge, little attention has been given to how this pretreatment affects the chemical composition and quality of the resulting bio-oil. Therefore, this study aims to systematically investigate the influence of pressurized air oxidation pretreatment on the pyrolysis behavior of lignocellulosic biomass, with a particular emphasis on product distribution and bio-oil quality. While slow pyrolysis was employed to analyze product trends, the findings are expected to inform future applications of fast pyrolysis, where both high yield and improved bio-oil composition are simultaneously desired.

MATERIALS AND METHODS

Materials

RS and EUCA were selected as the two biomass samples, derived from by-products of pulp mills and rice fields in Thailand. The raw biomass was first ground using a cutting mill and further reduced in size with a ball mill. The material was then sieved to obtain particles with an average diameter of approximately 1.5 mm, which were subsequently dried at 70 °C in a vacuum oven before the experiments. Table 1 presents the structural compositions of RS and EUCA, highlighting their significant differences.

Table 1. Structural composition of biomass.

Sample (Abbreviation)	Structural Composition [wt%, d.a.f.]			
	Cellulose	Hemicellulose	Lignin	Extractives
RS	33.5	43.8	16.5	6.2
EUCA	36.9	28.0	32.7	2.4

Pressurized Air Oxidation Process

Figure 1 presents a schematic diagram of the pressurized air oxidation process used to produce upgraded biomass. Biomass particles (1.5 mm in diameter) were processed in a 4 L batch autoclave reactor (Parr Instrument Company, Series 4848). Approximately 1000 g of biomass was used in each run. The sample was heated to 250 °C and held at that temperature for 30 mins under various gas pressures. Initial gas mixtures consisted of an O_2/He premix (22 vol.% O_2, balance He), selected to set the target oxygen partial pressure with an inert diluent and to ensure high compositional accuracy. Before heating, the reactor was pressurized to 0.5 or 1.0 MPa to control the internal reaction pressure. During the reaction, the final pressure ~ doubled, reaching ~1.0 and 2.0 MPa, respectively. For

atmospheric pressure pretreatment (0.1 MPa), the reactor valve was opened to allow continuous gas flow through the sample at a rate of 200 mL/min. All resulting products were collected and analyzed. Liquid products were obtained by washing with acetone, which was subsequently evaporated using a rotary evaporator. Gaseous products were collected in a gas bag. The remaining solid, referred to as "upgraded biomass," was dried and characterized by several techniques. To ensure the reproducibility and reliability of the data, all experiments were repeated at least three times, and the collected products were analyzed in subsequent procedures. The presented values correspond to the average of replicate measurements, with standard deviations included as indicators of experimental variability.

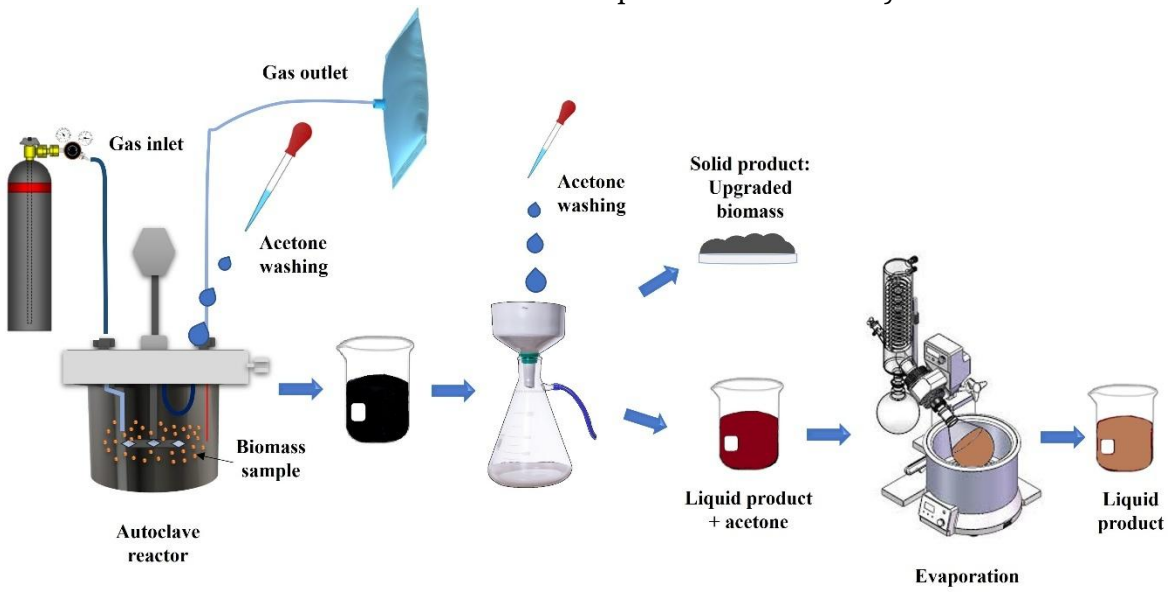

Figure 1. Schematic diagram of the experimental procedure for producing the upgraded biomass through a pressurized air oxidation treatment process.

In this study, abbreviations are used to indicate treatment conditions. For example, EUCA 250-1.0 refers to eucalyptus treated at 250 °C with an initial pressure of 1.0 MPa under pressurized air oxidation, while EUCA 250-0.1 refers to eucalyptus treated at 250 °C under atmospheric pressure.

Pyrolysis Experiments

Pyrolysis experiments were conducted in two phases: the first examined decomposition behavior, and the second produced bio-oil. For the decomposition analysis, thermogravimetric analysis (TGA 50H, Shimadzu) was used to monitor mass loss and assess the thermal degradation behavior. Approximately 10 mg of sample was heated under high-purity nitrogen (99.999%) at 10 °C/min from room temperature to 900 °C. The heating was extended to 900 °C to ensure complete thermal stabilization. However, the char yield was defined at 800 °C under N_2, which is a practical endpoint commonly adopted in biomass pyrolysis studies [28].

To complement the TGA results, a fixed-bed quartz tube reactor was employed to evaluate product distributions, especially the yield of bio-oil. In each experiment, approximately 60 g of biomass was loaded into a ceramic crucible positioned at the center of a horizontal cylindrical furnace, as illustrated in Figure 2. The reactor was purged with nitrogen at a flow rate of 200 mL/min for 20 mins to remove residual air, after which the sample was heated at a constant rate of 10 °C/min to 550 °C and held isothermally for 30 mins. A thermocouple located just above the crucible was used to monitor and control the reaction temperature. The condensable vapors were collected in ice-cooled condensers, while the bio-oil fraction was recovered for subsequent characterization. Non-condensable gases were collected in 10 L sampling bags and analyzed using a micro gas chromatograph (490 Micro GC, Agilent Technologies). After the reaction, the reactor was rapidly cooled under nitrogen flow, and the residual char was retrieved and weighed.

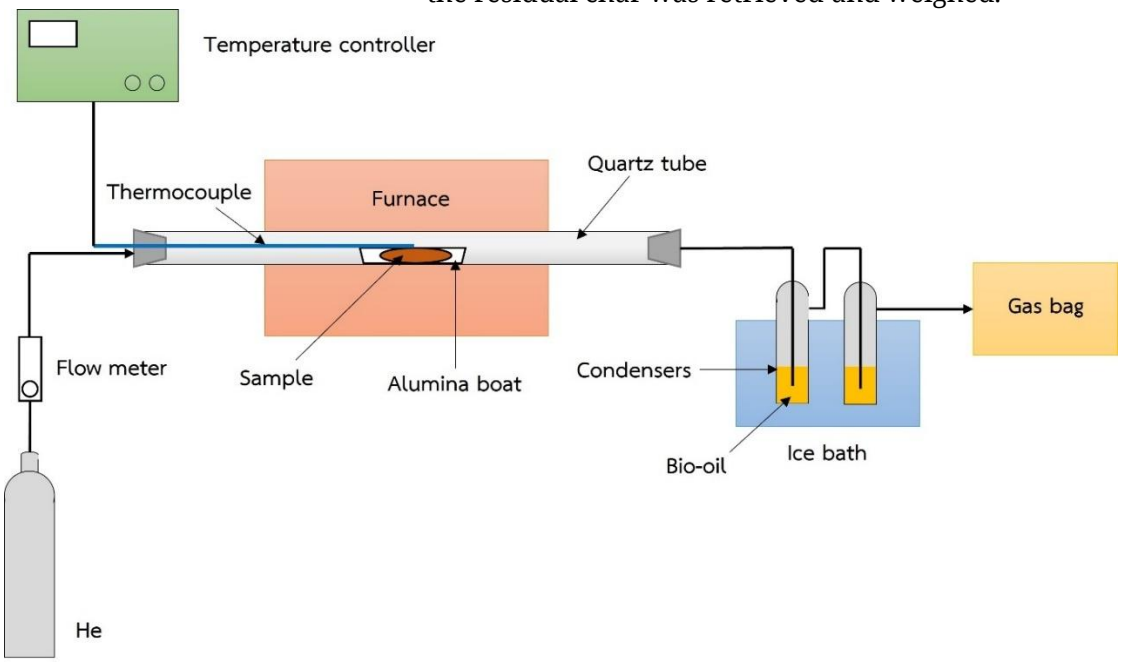

Figure 2. Schematic diagram of bio-oil production from the pyrolysis process.

It is important to note that the TGA and fixed-bed reactor experiments served complementary purposes and were conducted at different scales (mg vs. g). Accordingly, the results are interpreted in parallel, with emphasis on comparative trends rather than direct numerical equivalence. This distinction ensures consistency in interpreting the thermal decomposition behavior and product yields while recognizing the inherent differences between analytical and preparative scales.

Solid Product Analysis

Proximate Analysis

The proximate analysis of biomass and upgraded biomass was conducted using a thermogravimetric analyzer (TGA-50H, Shimadzu), following ASTM E1131. The sample was ground and sieved to obtain a particle size smaller than 75 μm in order to minimize heat and mass transfer limitations during thermal decomposition. Approximately 10 mg of the prepared sample was placed in a platinum crucible and analyzed under a constant gas flow of 50 mL/min. The heating program was as follows: initially, the sample was heated from ambient temperature to 110 °C and held isothermally for 15 mins under nitrogen to determine the moisture content. The temperature was then increased from 110 °C to 900 °C at a constant heating rate of 10 °C/min under nitrogen, and the mass loss in this stage was attributed to volatile matter. (In this study, volatile matter was defined as the mass loss under nitrogen up to 900 °C.) After reaching 900 °C, the purge gas was switched from nitrogen to Air Zero at the same flow rate, and heating was continued until the sample mass remained constant, allowing the determination of ash content. The fixed carbon fraction was calculated by difference, as the residue after subtracting moisture, volatile matter, and ash contents.

Ultimate Analysis

The ultimate (elemental) analysis was carried out using a CHN analyzer (CHN JM10, J-Science Lab). Approximately 2 mg of finely ground sample was used for each measurement. The instrument was calibrated with 2,5-bis(5-tert-butyl-2-benzoxazol-2-yl) thiophene (BBOT), a standard reference compound containing 72.58 wt% carbon, 6.10 wt% hydrogen, 6.53 wt% nitrogen, and 7.44 wt% sulfur.

Heating Value Analysis

The higher heating value (HHV) of the samples, calculated on a dry basis (d.b.) from the elemental analysis results using a Unified HHV Correlation [29], is expressed as follows:

$$\text{HHV (MJ/kg, d.b.)} = 0.3491C + 1.1783H + 0.1005S - 0.1034O - 0.0151N - 0.0211A \quad (1)$$

In this equation, *C*, *H*, *S*, *O*, *N*, and *A* represent the mass percentages of carbon, hydrogen, sulfur, oxygen, nitrogen, and ash, respectively.

Gas Product Analysis

Gas products were analyzed using a Micro GC (490 Micro GC, Agilent Technologies) equipped with a thermal conductivity detector (TCD). Helium was used as the balance/carrier gas for calibration and analysis. External standard calibrations were applied as follows: CO and CH_4 were quantified using a single-point calibration based on a standard He-balanced gas mixture (containing CO_2 1.2 vol%, CO 0.97 vol%, CH_4 1.1 vol%),

while CO_2 was quantified using a three-point calibration (1.2, 20.0, and 99.99 vol%) to ensure accuracy across the concentration range observed. Light hydrocarbons (C_2–C_4) were not analyzed in this study; under the present slow-pyrolysis conditions their concentrations are expected to be low and outside the reliable detection range of TCD.

Condensable Product Analysis (Bio-oil and Water)

The condensable fraction was separated into organic bio-oil and water components for analysis. The organic fraction was characterized using gas chromatography–mass spectrometry (GC–MS, GCMS-QP2010 SE, Shimadzu). Prior to analysis, bio-oil samples were diluted in isopropanol to a concentration of 1% (*v*/*v*). An aliquot of approximately 2 μg was injected in split mode. Separation was achieved on a DB-5MS capillary column (60 m × 0.32 mm i.d., 0.25 μm film thickness), with high-purity helium as the carrier gas at a constant flow rate of 1.0 mL/min. The oven temperature was programmed from ambient temperature to 300 °C at 5 °C/min, with both the injector and ion source maintained at 300 °C. The mass spectra were identified by comparison with the NIST library.

The water content of the condensable fraction was determined by Karl Fischer titration in accordance with ASTM D6304-20. Duplicate measurements were performed, and the average values were used in the analysis.

RESULTS AND DISCUSSION

Yields and Chemical Properties of Upgraded Biomass

Table 2 presents the yields and proximate analysis of RS, upgraded RS, EUCA, and upgraded EUCA, derived from the pressurized air oxidation process. It was observed that, on a dry weight basis, the pressurized oxidation process caused changes in both yield and chemical composition. Specifically, when treated at higher pressures, the yield generally increased. For instance, EUCA treated at 0.5 MPa yielded approximately 50.5 ± 1.3 wt.%, while treatment at 1.0 MPa resulted in a slightly lower yield of 44.9 ± 1.2 wt.%. In the case of RS, the yield increased with pressure, reaching 52.8 ± 1.1 wt.% at 1.0 MPa. The upgraded biomass exhibited higher fixed carbon and lower volatile matter compared to the raw biomass. These changes indicate partial devolatilization and carbon enrichment during the pressurized oxidation process. The fixed carbon content of upgraded EUCA increased from 14.1% (raw) to 64.2 wt.% at 0.5 MPa, while the volatile matter content decreased from 83.0 wt.% to 34.0 wt.%. Similar trends were observed in RS, where the fixed carbon increased from 13.2 wt.% (raw) to 46.7 wt.%, and the volatile matter decreased from 74.1 wt.% to 28.3 wt.%. Notably, the ash content of RS was significantly higher than that of EUCA, ranging from 25.0–35.2 wt.% for RS and only 0.9–2.1 wt.% for EUCA. These results suggest that the pressurized air oxidation process effectively improves the fuel properties of

lignocellulosic biomass by enhancing carbon content and reducing volatile components, particularly at moderate pressures.

Table 2. Proximate analysis and yield of biomass and upgraded biomass prepared from a pressurized air oxidation process.

Samples [°C-MPa]	Yield [wt.%, d.b.]	Moisture [wt.%, w.b.]	Proximate Analysis [wt.%, d.b.]		
			Volatile Matter	Fixed Carbon	Ash
RS	-	4.5	74.1	13.2	12.7
RS 250-0.1	44.7 ± 0.8	3.8	28.5	36.3	35.2
RS 250-0.5	50.6 ± 1.2	2.4	31.6	38.9	29.5
RS 250-1.0	52.8 ± 1.1	1.3	28.3	46.7	25.0
EUCA	-	4.4	83.0	14.1	0.9
EUCA 250-0.1	45.3 ± 0.9	4.5	47.7	50.3	2.0
EUCA 250-0.5	50.5 ± 1.3	2.4	34.0	64.2	1.8
EUCA 250-1.0	44.9 ± 1.2	1.4	35.5	62.4	2.1

Table 3 presents the elemental compositions, HHV, and atomic ratios (O/C and H/C) of raw and upgraded biomass subjected to pressurized air oxidation. The results reveal clear evidence of chemical transformation, particularly in RS and EUCA, under varying oxidation pressures.

Table 3. Elemental compositions, HHV, atomic ratio of biomass, and upgraded biomass prepared from a pressurized air oxidation process.

Samples	Elemental Compositions [%, d.b.]				O/C	H/C	HHV
[°C-MPa]	C	H	N	O *	[-]	[-]	[MJ/kg, d.b.]
RS	41.6	6.4	1.1	38.2	0.69	1.84	17.81
RS 250-0.1	39.3	2.6	1.5	21.5	0.41	0.80	13.77
RS 250-0.5	46.3	3.5	1.5	19.2	0.31	0.90	17.70
RS 250-1.0	49.6	3.8	1.5	20.2	0.31	0.91	19.08
EUCA	48.3	6.8	0.4	43.7	0.68	1.68	20.28
EUCA 250-0.1	63.3	3.7	0.6	30.5	0.36	0.69	23.18
EUCA 250-0.5	66.8	4.8	0.6	26.0	0.29	0.86	26.21
EUCA 250-1.0	69.1	4.2	0.6	24.1	0.26	0.73	26.51

* Calculated from the difference, O/C and H/C atomic ratios were derived from dry ash-free data

For RS, the carbon content increased from 41.6 wt.% in the raw sample to 49.6 wt.% after treatment at 1.0 MPa, while the oxygen content decreased significantly from 38.2 wt.% to 20.2 wt.%. These changes resulted in a notable reduction in the O/C atomic ratio, from 0.69 to 0.31, and the H/C ratio, from 1.84 to 0.91. These transformations suggest increased aromaticity and structural condensation within the biomass matrix, contributing to improved thermal stability. As a result, the HHV increased from 17.81 MJ/kg to 19.08 MJ/kg, representing a 7.1% improvement in energy content.

For EUCA, a similar but more pronounced trend was observed. The carbon content increased substantially from 48.3% to 69.1 wt.%, while the oxygen content decreased from 43.7 wt.% to 24.1 wt.% at a pressure of 1.0 MPa. The corresponding O/C and H/C atomic ratios decreased from 0.68 to 0.26 and from 1.68 to 0.73, respectively. These compositional changes—including the consistent reduction in O/C atomic ratio and the initial decrease in H/C ratio—suggest the formation of more condensed aromatic

structures and thermally stable carbon. While the H/C ratio for EUCA showed a slight increase at higher pressures, the values remained significantly lower than in raw samples, supporting the overall trend toward enhanced aromaticity and thermal stability. Consequently, the HHV increased markedly from 20.28 MJ/kg to 26.51 MJ/kg—a 30.7% enhancement. Notably, significant improvement was already evident at 0.5 MPa (HHV: 29.2 MJ/kg), emphasizing the effectiveness of moderate-pressure oxidation.

To better visualize these trends, a van Krevelen diagram is shown in Figure 3. Both upgraded RS and EUCA move toward the lower-left region (decreasing O/C and H/C), lying closest to the $-H_2O$ trajectory. This net downward-left displacement indicates that dehydration accompanied by dehydrogenation/condensation (aromatization) is the prevailing transformation during pressurized-air pretreatment. As the pretreatment pressure increases (0.1 → 0.5 → 1.0 MPa), the points shift further left and—particularly for RS—slightly upward, a pattern consistent with a growing contribution from decarboxylation ($-CO_2$). The pressure-induced changes are modest overall and become minor for EUCA beyond 0.5 MPa. These vectorial shifts are consistent with the pressure-dependent elemental trends reported earlier.

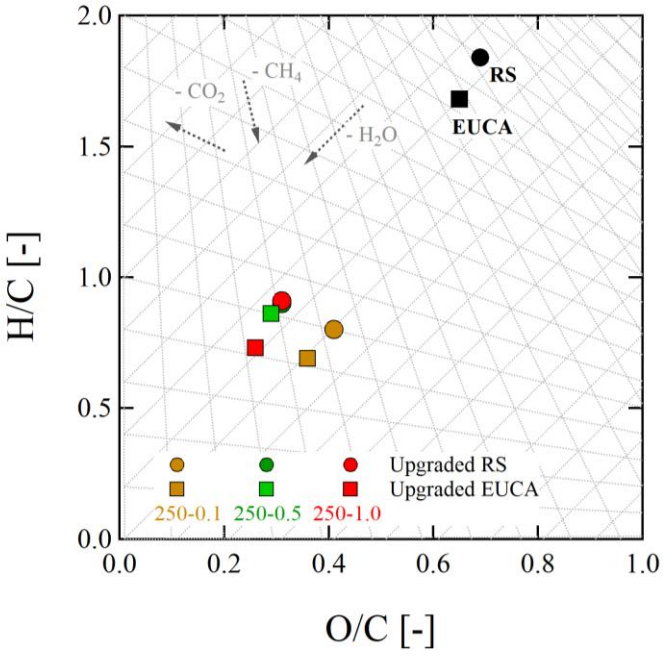

Figure 3. van Krevelen diagram for raw and upgraded RS and EUCA after pressurized-air pretreatment at 250 °C (0.1, 0.5, 1.0 MPa). Diagonal lines indicate the main reaction pathways during thermal degradation: dehydration ($-H_2O$), decarboxylation ($-CO_2$), and demethanation ($-CH_4$).

Consistent with the van Krevelen analysis (Figure 3), the observed carbon enrichment and the concurrent decreases in H/C and O/C are comparable to trends reported for systems dominated by dehydration and decarboxylation reactions, such as hydrothermal carbonization [30,31], pressurized torrefaction [24,25], and degradative solvent extraction [32,33], although the underlying mechanisms differ considerably. While

the chemical environment under pressurized air oxidation is distinct from these processes, the resultant elemental trends suggest that analogous pathways—particularly the cleavage of hydroxyl and carboxyl functionalities—may also occur under mildly oxidative conditions. Nonetheless, as pressurized air oxidation remains a relatively new pretreatment technique, further studies are warranted to elucidate its structural and mechanistic transformations in greater detail.

Pyrolysis Behaviors of Upgraded Biomass

The pyrolysis behavior of raw and upgraded biomass samples was investigated using thermogravimetric analysis (TGA) under a nitrogen atmosphere at a constant heating rate of 10 °C/min. All results are expressed on a dry and ash-free (d.a.f.) basis to eliminate the influence of ash. This approach ensures that the data reflect only the decomposition of organic matter, allowing for a consistent comparison of char formation among different samples. In addition, all TGA curves are normalized to the initial dry, ash-free mass of the raw biomass; for upgraded samples, the starting point equals the pretreatment solid yield (Table 1).

Figure 4 shows the TGA curves of raw RS and upgraded RS pretreated at 250 °C under varying initial pressures (0.1–1.0 MPa). The upgraded RS samples retained significantly more char than raw RS, particularly at temperatures above 400 °C. For example, the RS pretreated at 1.0 MPa yielded 31 wt.% char at 800 °C, compared to only 19 wt.% for raw RS. The char yield increased progressively with pressure from 0.1 to 1.0 MPa (19.3, 25.3, and 26.8 wt.%, respectively). This trend suggests that moderate pressure enables partial oxidation, combined with condensation reactions, promoting the formation of a thermally stable, cross-linked carbon matrix that is resistant to devolatilization. Previous studies have also shown that pressurized torrefaction can enhance char formation. For instance, torrefaction of compressed samples under mechanical load (10–70 MPa, 250 °C) was reported to increase char yield at high pyrolysis temperatures [26], while gas-pressurized torrefaction improved solid retention and subsequently led to higher char yields during pyrolysis [27]. Together, these results suggest that both mechanical and gas pressurization promote cross-linking reactions and suppress devolatilization, thereby enhancing char retention compared to torrefaction at atmospheric pressure. Overall, the present study confirms that pretreatment pressure exerts a significant influence on char formation during thermal decomposition.

Figure 5 presents the TGA curves of raw and upgraded EUCA subjected to the same pyrolysis conditions. All upgraded EUCA samples exhibited higher char yields than raw EUCA. The maximum char yield (31.8 wt.%) was obtained from the sample pretreated at 0.5 MPa, followed by 29.3 wt.% at 1.0 MPa. The consistently higher char yields observed in EUCA compared to RS under identical pretreatment conditions can be primarily attributed to differences in structural composition, particularly lignin content. EUCA typically contains a higher lignin fraction (32.7 wt%) than

rice straw (16.5 wt%), as shown in Table 1. Although lignin begins to decompose at relatively low temperatures (150–175 °C), its degradation proceeds more gradually over a much broader temperature window than cellulose and hemicellulose. Consequently, lignin-rich feedstocks retain more solid residues at elevated temperatures and produce more condensed, aromatic char, which is associated with higher thermal stability [34–36]. This helps explain the higher char yields observed for EUCA (higher lignin) relative to RS.

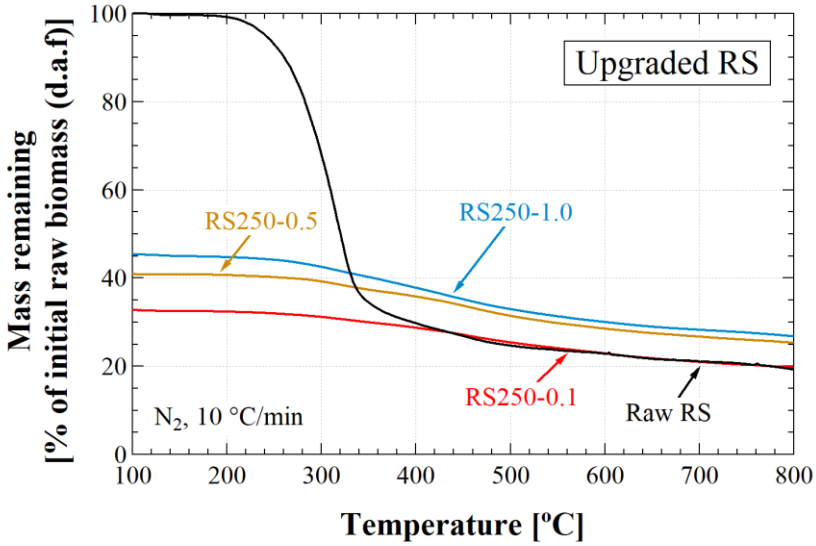

Figure 4. TGA curves during pyrolysis of RS and upgraded RS prepared at various pressures.

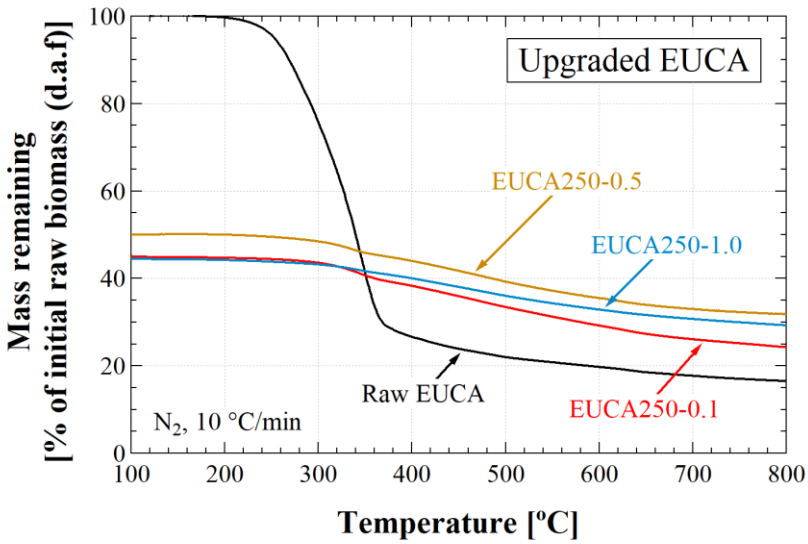

Figure 5. TGA curve during pyrolysis of raw EUCA and upgraded EUCA prepared at various pressures.

Furthermore, the upgraded biomass samples exhibited slower mass loss rates in the high-temperature region (>400 °C), corresponding to the carbonization stage. This behavior indicates increased resistance to devolatilization, likely due to the development of condensed aromatic domains during pressurized oxidation. The effect was more pronounced in samples treated at moderate pressures, further supporting the hypothesis that pressure-induced structural condensation occurs.

Product Distribution Obtained from Pyrolysis of Upgraded Biomass

This section investigates the production of bio-oil via pyrolysis using a fixed-bed system operated at 550 °C for 30 mins. Both raw and upgraded biomass samples, prepared under atmospheric and pressurized conditions, were compared. For RS, the RS250-1.0 sample was selected to represent the high-pressure condition, as it exhibited both the highest product yield and heating value. For EUCA, the EUCA250-0.5 condition was chosen due to its optimal balance of product yield (50.53 wt.%) and heating value, which is comparable to the 1.0 MPa condition. These selected conditions were used for comparison with the corresponding raw biomass samples in the subsequent analysis. It should be noted that the reported bio-oil yields were obtained from mass balances of the quantified products for both RS and EUCA. Light hydrocarbons (C_2–C_4) were not quantified in this study; however, their contribution under slow pyrolysis at 550 °C is generally minor and unlikely to affect the comparative trends presented.

Figure 6a illustrates the product distribution from RS and upgraded RS. Raw RS produced 36.9 wt.% char, 28.7 wt.% bio-oil, 13.6 wt.% water, and 11.6 wt.% CO_2, together with minor amounts of CO and CH_4. After upgrading at 0.1 MPa, the char yield increased markedly to 78.4 wt.%, while the bio-oil yield declined to 2.4 wt.%, reflecting a strong suppression of volatile release. This trend is consistent with partial oxidative decomposition of volatiles during pretreatment, as later discussed in the mechanistic interpretation below. At 1.0 MPa, the char yield slightly decreased to 76.4 wt.%, whereas the bio-oil yield partially recovered to 7.9 wt.%. The modest increase in liquid production at elevated pressure may be attributed to the enhanced condensation of heavier hydrocarbon compounds. Although the overall bio-oil yield was relatively low under slow pyrolysis conditions, this operating regime was intentionally selected to isolate and evaluate the effects of pretreatment pressure on product distribution.

It is noteworthy that the condensable fraction comprised both organic bio-oil and reaction water, with water accounting for approximately one-third of the total condensable. A slight decreasing trend in the relative water content was observed with increasing pretreatment pressure: in RS, the proportion decreased from ~32.3 wt.% in the raw sample to ~30.1 wt.% in RS 250–1.0. Although the reduction is modest, it suggests a subtle but consistent trend toward lower water content in the condensable fraction under oxidative pretreatment. This observation may indicate a marginal improvement in the quality of the condensable liquids, as a reduced water fraction is generally considered more favorable for the subsequent utilization of bio-oil.

Figure 6b shows the corresponding results for EUCA. Raw EUCA produced 27.8 wt.% char, 39.9 wt.% bio-oil, and 18.4 wt.% water, with CO_2 as the dominant gaseous product (9.4 wt.%). Following pretreatment at 0.1 MPa (EUCA 250–0.1), the char yield increased substantially, while the bio-oil yield decreased to 7.6 wt.%. At 0.5 MPa (EUCA 250–0.5), the bio-oil yield

improved slightly to 9.4 wt.%, consistent with more effective condensation of partially oxidized intermediates under moderate pressure. Across all conditions, EUCA still delivered higher liquid yields than RS. The water fraction of the condensables decreased marginally (~31.5 → ~30.1 wt.%), indicating a small improvement in condensable quality. Although this reduction is minor, it suggests a modest yet favorable shift toward improved condensable quality, as excessive water content is generally considered detrimental to the heating value and stability of pyrolysis liquids. Beyond this observation, a comparative analysis further highlights the impact of biomass type on product distribution. Raw EUCA consistently exhibited a markedly higher bio-oil yield compared to RS, a difference that can be primarily attributed to its higher volatile content and lower ash content. Taken together, these findings indicate that both the pretreatment pressure and the intrinsic feedstock characteristics jointly govern the yield and quality of condensable products during pyrolysis.

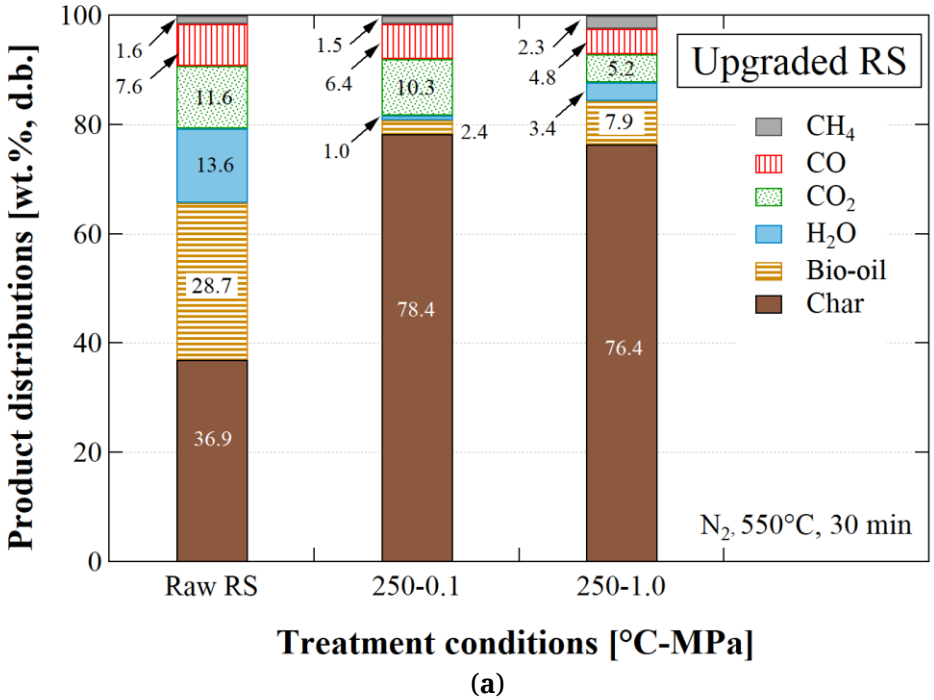

(a)

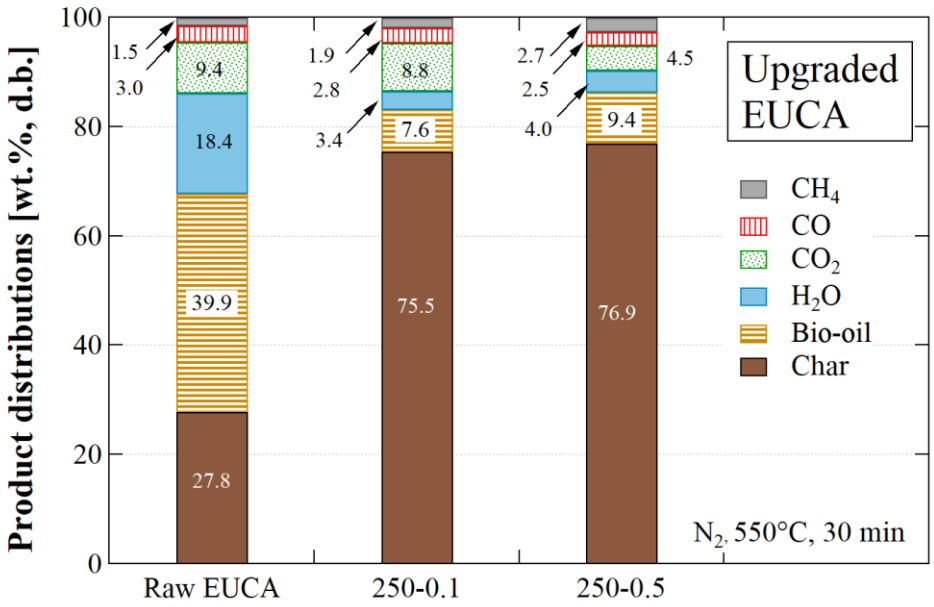

(b)

Figure 6. Production distributions throughout the pyrolysis at 550 °C, 30 mins for (**a**) RS and upgraded RS and (**b**) EUCA and upgraded EUCA.

The substantial reduction in liquid yield after pressurized-air pretreatment (raw ≈ 30–40 wt.% → ≈ 2–10 wt.% at 0.1–1.0 MPa, Figure 5) has been suggested in the literature to involve: (i) oxidative conversion of volatile components into non-condensable gases, (ii) partial oxidation toward more stable, oxygen-depleted intermediates, and (iii) structural rearrangement/aromatization that favors char formation. While direct mechanistic evidence under the present conditions remains unavailable, these concurrent effects plausibly account for the marked drop, whereas the modest recovery near 1.0 MPa (≈9–10 wt.% for both RS and EUCA) may reflect improved condensation of heavier, less-oxygenated compounds; alternative explanations (e.g., over-oxidation/secondary reactions at lower pressure) cannot be ruled out. Overall, the results indicate a yield–quality trade-off: pretreatment can improve the chemical quality/stability of condensables (Section 3.4) yet simultaneously reduce total liquid yield, which should be balanced in process optimization.

Chemical Compositions of Condensable Liquids Produced from Upgraded Biomass

The condensable liquids collected from RS, upgraded RS, EUCA, and upgraded EUCA were analyzed to evaluate the influence of oxidative pretreatment on chemical composition. As shown in Figures 7 and 8, the condensable liquids derived from the upgraded RS exhibited a slightly higher intensity of chromatographic peaks compared with raw RS, indicating subtle but discernible shifts in chemical composition. In contrast, the upgraded EUCA bio-oil showed a modest reduction in peak

intensity relative to raw EUCA, suggesting that pretreatment promoted partial stabilization of intermediates, leading to fewer detectable compounds.

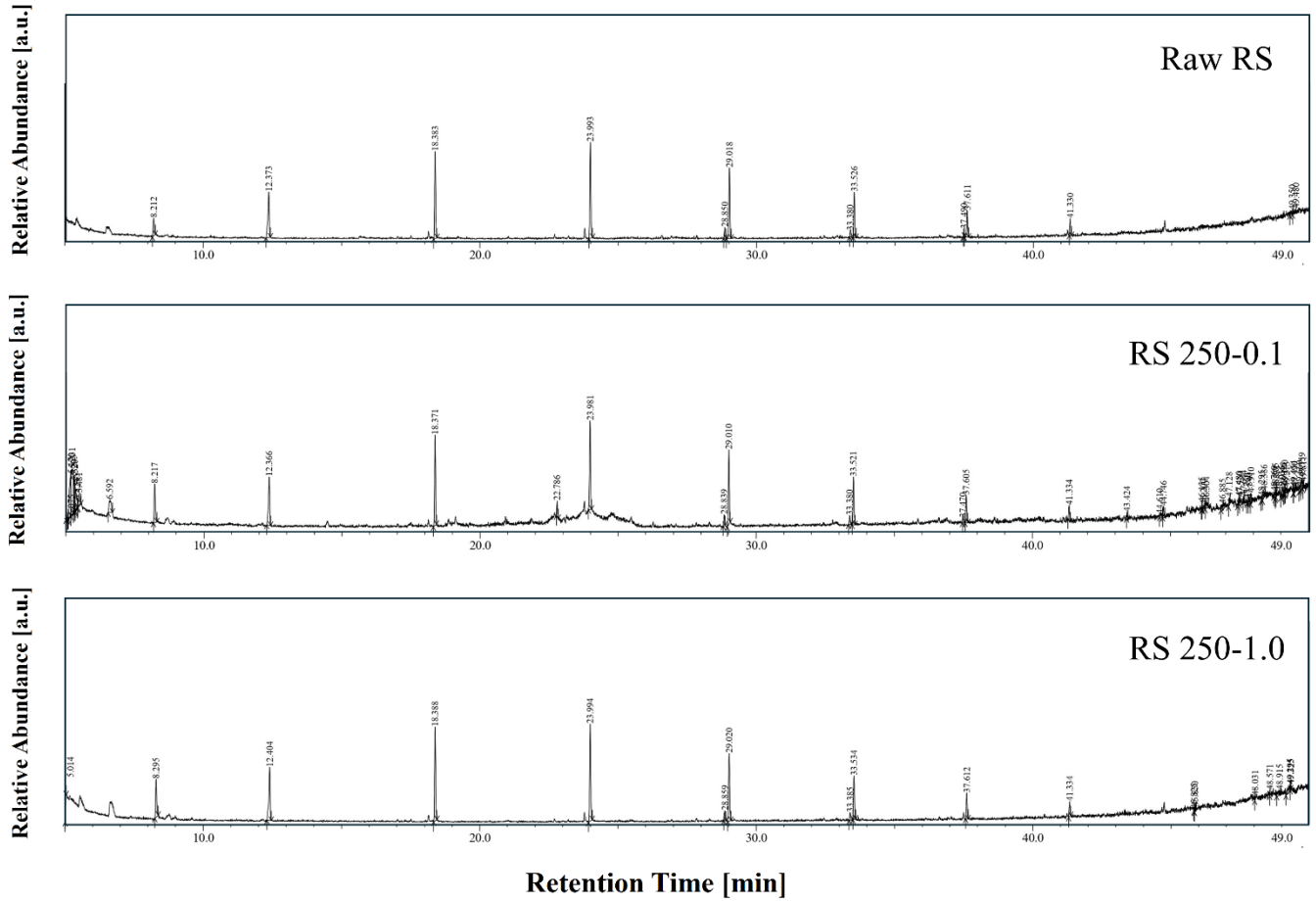

Figure 7. GC-MS Chromatograms of bio-oils produced from RS and upgraded RS prepared under various pressures.

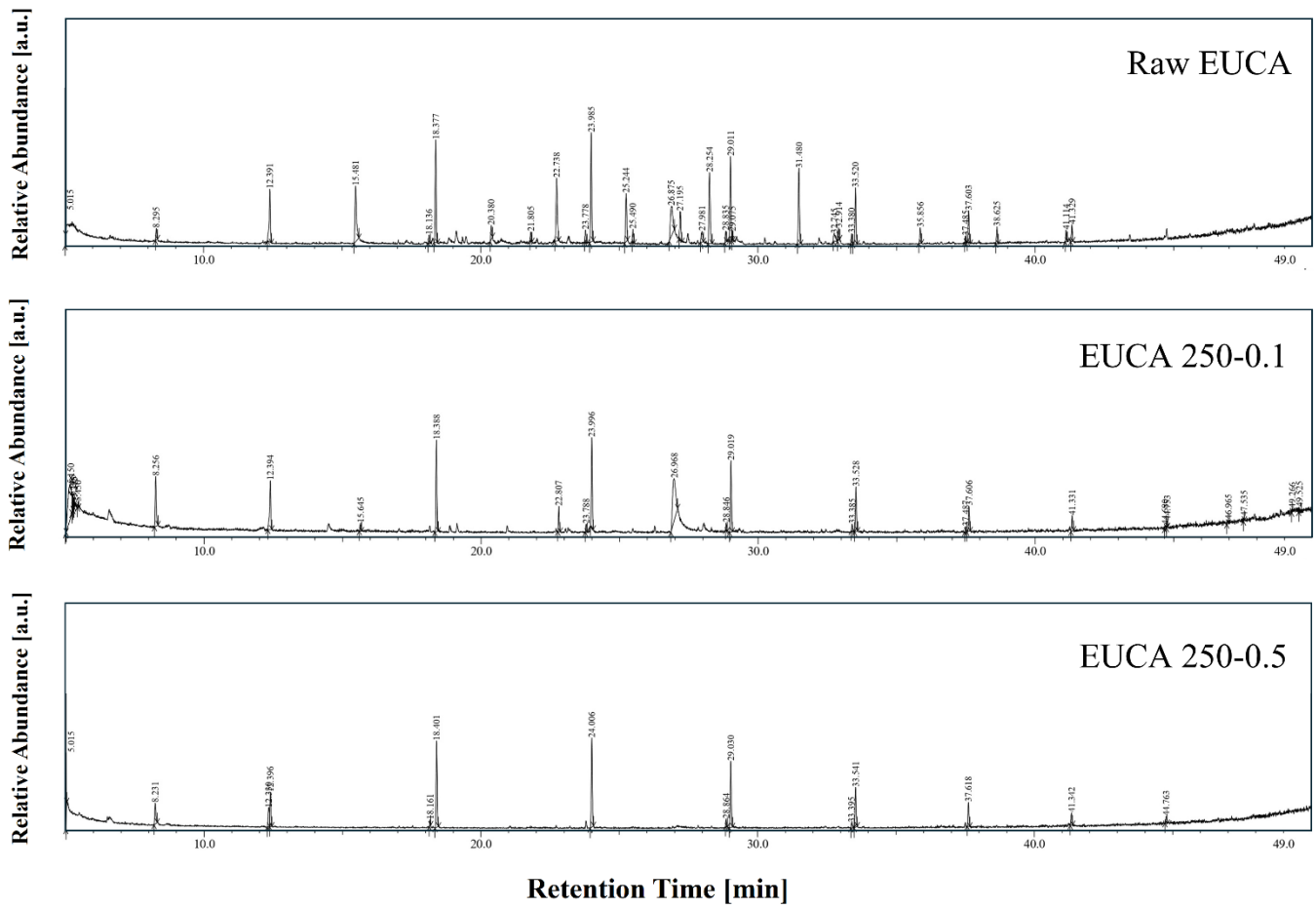

Figure 8. GC-MS Chromatograms of bio-oils produced from EUCA and upgraded EUCA prepared under various pressures.

Figure 9 summarizes the functional-group distributions of the condensable products for the biomass and their upgraded counterparts, based on GC-MS peak areas normalized to the sum of identified compounds. The condensable are grouped as alkanes, alkenes, aromatics, and esters, with minor alcohols; remaining species are reported as others.

For RS, the aromatic/phenolic fraction decreases with pretreatment pressure, whereas alkanes become relatively enriched—consistent with the emergence or growth of long-chain paraffins after pretreatment and subsequent pyrolysis. Ester/ketone features show a modest variation with pressure, peaking slightly at 0.1 MPa, then declining at 1.0 MPa. At the same time, alcohols/alkenes remain at low levels. Overall, RS exhibits a group-level shift from oxygenates toward saturated hydrocarbons with increasing pressure.

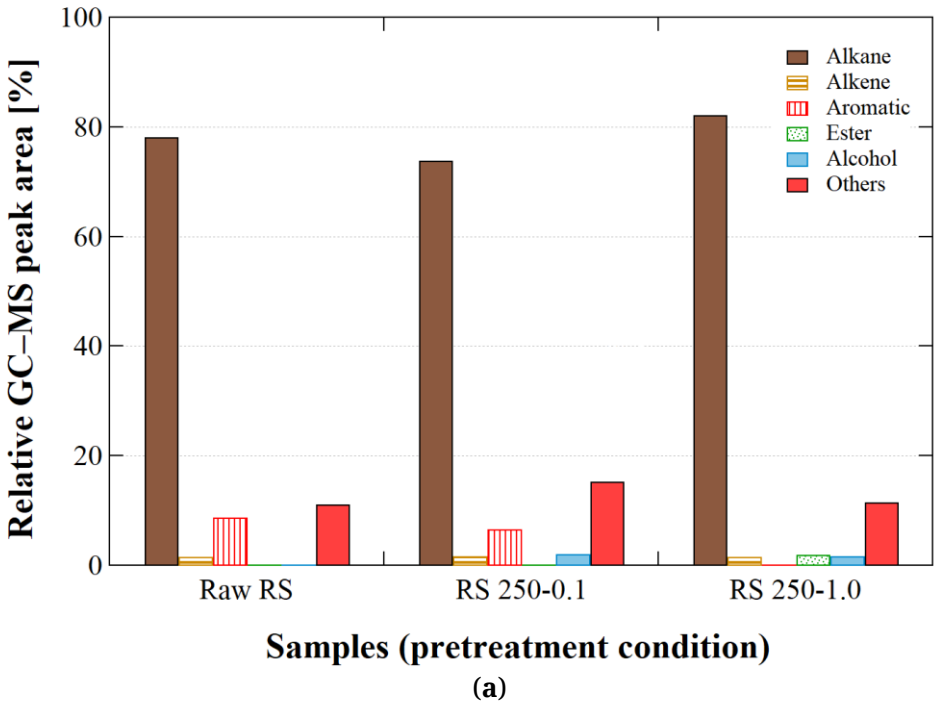

Figure 9. Functional-group distributions of bio-oils (relative GC-MS peak area, normalized to the sum of identified compounds) produced from (**a**) RS and upgraded RS and (**b**) EUCA and upgraded EUCA.

For EUCA, the alkane fraction increases markedly with pretreatment (from ~42% to >80% at 0.5 MPa), while aromatics become undetectable. The ester and others classes increase at 0.1 MPa and decline at 0.5 MPa.

Tables 4 and 5 provide the compound-level compositions that underpin these trends. For RS (Table 4), toluene decreases from 8.86% (raw) to 6.73% (0.1 MPa) and is undetected at 1.0 MPa. In parallel, straight-chain alkanes strengthen: decane appears only at 1.0 MPa (14.02%), dodecane remains abundant though slightly declining (23.14 → 21.97 → 19.05%). Octadecane

was not detected after pretreatment. Several oxygenates vary non-monotonically (e.g., 2-pentanone, 4-hydroxy-4-methyl- peaks at 10.18% at 0.1 MPa; 1-undecanol emerges only after pretreatment). These observations illustrate the suppression of aromatics and a shift toward long-chain aliphatic hydrocarbons at higher pressure, while some aliphatics decline slightly.

Table 4. Chemical composition of bio-oils produced from RS and upgraded RS under various preparation conditions.

Retention Time	Compounds Name	% Area		
		RS	RS 250-0.1	RS 250-1.0
5.014	2-Propanone, 1-methoxy-	1.02	0.00	3.64
6.592	Toluene	8.86	6.73	0.00
8.217	2-Pentanone, 4-hydroxy-4-methyl-	6.74	10.18	7.95
12.366	Nonane, 2-methyl-	16.1	13.61	0.00
12.404	Decane	0.00	0.00	14.02
18.371	Dodecane	23.14	21.97	19.05
23.994	Tetradecane	0	0.00	20.12
28.839	1-Undecanol	0	2.16	1.82
28.85	unknown	2.43	0.00	0.00
29.01	Pentadecane	0.00	17.66	0.00
29.02	2,6-Dimethyltridecane	15.67	0.00	14.84
33.38	1-Undecene, 9-methyl-	1.7	1.82	1.65
33.521	Nonadecane, 2-methyl-	12.74	11.36	9.12
37.49	unidentified aliphatic	1.05	1.77	0.00
37.605	Heptadecane	0.00	6.78	0.00
37.611	Undecane, 3,8-dimethyl-	6.71	0.00	5.11
41.33	Octadecane	3.28	0.00	0.00
41.334	C18–C19 aliphatic	0.00	3.36	0.00
44.746	Nonadecane	0.56	2.6	0.00

Table 5. Chemical composition of bio-oils produced from EUCA and upgraded EUCA under various preparation conditions.

Retention Time	Compounds Name	% Area		
		EUCA	EUCA 250-0.1	EUCA 250-0.5
5.015	Hydroperoxide, 1-methylpentyl	0.78	12.27	4.33
5.15	8,11-Octadecadiynoic acid, methyl ester	0.00	14.95	0.00
8.295	2-Pentanone, 4-hydroxy-4-methyl-	0.98	6.54	5.54
12.33	Octane, 2,7-dimethyl-	0.00	0.00	5.44
12.391	Nonane, 2-methyl-	5.83	7.18	7.55
15.481	Cyclopropyl carbinol	8.13	0.00	0.00
18.161	Cyclopentane, 1,1,3-trimethyl-	0.00	0.00	0.76
18.136	1-Heptanol, 6-methyl-	0.55	0.00	0.00
18.377	Dodecane	9.68	10.90	19.47
20.38	1,2-Benzenediol, 3-methoxy-	1.26	0.00	0.00
21.805	2-Methoxy-4-vinylphenol	0.69	0.00	0.00
22.738	Phenol, 2,6-dimethoxy-	7.83	0.00	0.00
23.778	1-Dodecene	1.13	0.00	0.00
23.985	Tetradecane	10.45	10.81	20.63
25.244	3,5-Dimethoxy-4-hydroxytoluene	5.15	0.00	0.00
25.49	Phenol, 2-methoxy-4-(1-propenyl)-	1.01	0.00	0.00
26.875	D-Allose	6.37	15.72	0.00
27.195	5-tert-Butylpyrogallol	3.10	0.00	0.00
27.981	2-Cyclopenten-1-one, 3-(acetyloxy)-	1.47	0.00	0.00
28.254	3',5'-Dimethoxyacetophenone	8.28	0.00	0.00
28.846	1-Heptanol, 6-methyl-	0.00	0.71	0.00
28.864	1-Decene, 8-methyl-	0.00	0.00	1.13
29.011	Pentadecane	7.63	8.83	15.16

31.48	Phenol, 2,6-dimethoxy-4-(2-propenyl)-	8.60	0.00	0.00
32.745	Cyclohexasiloxane, dodecamethyl-	1.26	0.00	0.00
32.914	2-Pentanone, 1-(2,4,6-trihydroxyphenyl)	1.14	0.00	0.00
33.38	1-Undecene, 9-methyl-	0.78	0.61	0.00
33.395	1-Pentanol, 3,4-dimethyl-	0.00	0.00	1.27
33.52	Nonadecane, 2-methyl-	5.03	5.40	9.29
37.487	unidentified aliphatic	0.00	0.55	0.00
37.603	Heptadecane	2.89	3.00	5.26
41.331	Octadecane	0.00	1.82	2.63

For EUCA (Table 5), lignin-derived methoxy-phenolics present in the raw oil (e.g., 2,6-dimethoxyphenol 7.83%, 2-methoxy-4-(1-propenyl)phenol 1.01%, 3,5-dimethoxy-4-hydroxytoluene 5.15%) disappear after pretreatment, while long-chain alkanes rise strongly: dodecane 9.68 → 10.90 → 19.47%, tetradecane 10.45 → 10.81 → 20.63%, pentadecane 7.63 → 8.83 → 15.16% (raw → 0.1 → 0.5 MPa). Transient oxygenates (e.g., hydroperoxide, 1-methylpentyl 12.27%; methyl 8,11-octadecadiynoate 14.95%) appear at 0.1 MPa but recede at 0.5 MPa. Together, EUCA shows a clearer shift toward long-chain aliphatics with suppression of phenolics/sugar-like species as pressure increases.

Across both feedstocks, pressurized-air pretreatment at 250 °C promotes deoxygenation of the condensable fraction—aromatics/oxygenates decline whereas paraffins increase in relative abundance. This pattern is consistent with the earlier elemental trends (lower O/C and H/C ratios) and with the measured slight decrease of the condensable water fraction (Table 5/Figure 3). Taken together, these composition-based indications point to a modest improvement in condensable quality under the studied conditions.

CONCLUSIONS

The present work provides a comprehensive evaluation of pressurized air oxidation as a pretreatment strategy for lignocellulosic biomass, extending the operating range to 1.0 MPa at relatively low temperatures (<250 °C). The results demonstrate that moderate pressures (0.5–1.0 MPa) substantially enhance carbon enrichment and improve the thermal stability of the upgraded solid fraction. In parallel, the condensable products were found to contain fewer oxygenated compounds and an increased proportion of long-chain aliphatic hydrocarbons, such as dodecane and pentadecane, indicating effective deoxygenation and improved chemical stability. While a decrease in bio-oil yield was observed with increasing pretreatment severity, this yield–quality trade-off highlights the need to balance condensable quality with overall liquid yield when optimizing the process. Importantly, this study provides the first systematic evidence linking pressurized-air oxidation with bio-oil composition, bridging a critical knowledge gap in the literature, which has primarily focused on the solid fraction.

Overall, the findings highlight the potential of pressurized air oxidation as a practical and scalable biomass upgrading method. By improving both solid and liquid pyrolysis products, this approach offers valuable insights for the development of future fast pyrolysis applications, where

simultaneously achieving high yield and enhanced bio-oil quality remains a key challenge.

DATA AVAILABILITY

The datasets generated and analyzed during the current study are available from the corresponding author upon reasonable request.

AUTHOR CONTRIBUTIONS

Conceptualization, PL and JW; methodology, PL and JW; formal analysis, TH and SJ; investigation, TH and SJ; resources, PL; data curation, TH and SJ; writing—original draft preparation, JW and SJ; writing—review and editing, JW and SJ; supervision, PL; project administration, PL; funding acquisition, PL. All authors have read and agreed to the published version of the manuscript.

CONFLICTS OF INTEREST

The authors declare that there are no conflicts of interest.

FUNDING

This research was funded by Suranaree University of Technology (SUT), Thailand Science Research and Innovation (TSRI), and the National Science Research and Innovation Fund (NSRF), grant number 195664.

ACKNOWLEDGEMENT

The authors would like to thank Navadol Laosiripojana from the Joint Graduate School of Energy and Environment, King Mongkut's University of Technology Thonburi, Bangkok, for supporting the apparatus used in this research.

REFERENCES

1. Neves D, Thunman H, Matos A, Tarelho L, Gómez-Barea A. Characterization and prediction of biomass pyrolysis products. Prog Energy Combust Sci. 2011;37:611-30. doi: 10.1016/j.pecs.2011.01.001.
2. Bridgwater AV. Review of fast pyrolysis of biomass and product upgrading. Biomass Bioenergy. 2012;38:68-94. doi: 10.1016/j.biombioe.2011.01.048.
3. Panwar NL, Divyangkumar N. An overview of recent advancements in biomass torrefaction. Environ Dev Sustain. 2024. doi: 10.1007/s10668-024-05623-0.
4. Zhang C, Chen W-H, Ho S-H, Zhang Y, Lim S. Comparative advantages analysis of oxidative torrefaction for solid biofuel production and property upgrading. Bioresour Technol. 2023;386:129531. doi: 10.1016/j.biortech.2023.129531.
5. Lilavanichakul A, Yoksan R. Development of bioplastics from cassava toward the sustainability of cassava value chain in Thailand. Sustainability. 2023;15:14713. doi: 10.3390/su152014713.

6. Lyu G, Wu S, Zhang H. Estimation and comparison of bio-oil components from different pyrolysis conditions. Front Energy Res. 2015;3:28. doi: 10.3389/fenrg.2015.00028.
7. Oasmaa A, Czernik S. Fuel oil quality of biomass pyrolysis oils: State of the art for the end users. Energy & Fuels. 1999;13:914-21. doi: 10.1021/ef980272b.
8. Bach Q-V, Tran K-Q, Khalil RA, Skreiberg Ø, Seisenbaeva G. Comparative assessment of wet torrefaction. Energy & Fuels. 2013;27:6743-53. doi: 10.1021/ef401295w.
9. Yang Z, Kumar A, Huhnke RL. Review of recent developments to improve storage and transportation stability of bio-oil. Renew Sustain Energy Rev. 2015;50:859-70. doi: 10.1016/j.rser.2015.05.025.
10. Khosravanipour Mostafazadeh A, Solomatnikova O, Drogui P, Tyagi RD. A review of recent research and developments in fast pyrolysis and bio-oil upgrading. Biomass Convers Biorefin. 2018;8:739-73. doi: 10.1007/s13399-018-0320-z.
11. Trinh QT, Banerjee A, Ansari KB, Dao DQ, Drif A, Binh NT, et al. Upgrading of bio-oil from biomass pyrolysis: Current status and future development. In: Biorefinery of alternative resources: Targeting green fuels and platform chemicals. Singapore: Springer; 2020. p. 317-53. doi: 10.1007/978-981-15-1804-1_14.
12. Mortensen PM, Grunwaldt J-D, Jensen PA, Knudsen KG, Jensen AD. A review of catalytic upgrading of bio-oil to engine fuels. Appl Catal A Gen. 2011;407:1-19. doi: 10.1016/j.apcata.2011.08.046.
13. Gea S, Hutapea YA, Piliang AFR, Pulungan AN, Rahayu R, Layla J, et al. A comprehensive review of experimental parameters in bio-oil upgrading from pyrolysis of biomass to biofuel through catalytic hydrodeoxygenation. Bioenergy Res. 2023;16:325-47. doi: 10.1007/s12155-022-10438-w.
14. Pimsamarn J, Kaewtrakulchai N, Wisetsai A, Mualchontham J, Muidaeng N, Jiraphothikul P, et al. Torrefaction of durian peel in air and N2 atmospheres: Impact on chemical properties and optimization of energy yield using multilevel factorial design. Res Eng. 2024;23:102767. doi: 10.1016/j.rineng.2024.102767.
15. Acharya B, Sule I, Dutta A. A review on advances of torrefaction technologies for biomass processing. Biomass Convers Biorefin. 2012;2:349-69. doi: 10.1007/s13399-012-0058-y.
16. Shankar Tumuluru J, Sokhansanj S, Hess JR, Wright CT, Boardman RD. Review: A review on biomass torrefaction process and product properties for energy applications. Ind Biotechnol. 2011;7:384-401. doi: 10.1089/ind.2011.7.384.
17. Devaraja UMA, Dissanayake CLW, Gunarathne DS, Chen W-H. Oxidative torrefaction and torrefaction-based biorefining of biomass: A critical review. Biof Res J. 2022;9:1672-96. doi: 10.18331/BRJ2022.9.3.4.
18. Chen D, Chen F, Cen K, Cao X, Zhang J, Zhou J. Upgrading rice husk via oxidative torrefaction: Characterization of solid, liquid, gaseous products and a comparison with non-oxidative torrefaction. Fuel. 2020;275:117936. doi: 10.1016/j.fuel.2020.117936.

19. Leontiev A, Kichatov B, Korshunov A, Kiverin A, Zaichenko V, Sytchev G, et al. Oxidative torrefaction of pine pellets in the quiescent layer of mineral filler. Fuel Process Technol. 2018;182:113-22. doi: 10.1016/j.fuproc.2018.10.021.
20. Jadsadajerm S, Wannapeera J, Phopiyanukror A, Worasuwannarak N. Influence of oxygen concentration on torrefaction of leucaena: Gas formation rates and chemical properties analysis. Biomass Convers Biorefin. 2025;15:7989-99. doi: 10.1007/s13399-024-05589-z.
21. Wang Q, Sun S, Zhang X, Liu H, Sun B, Guo S. Influence of air oxidative and non-oxidative torrefaction on the chemical properties of corn stalk. Bioresour Technol. 2021;332:125120. doi: 10.1016/j.biortech.2021.125120.
22. Nhuchhen DR, Basu P. Experimental investigation of mildly pressurized torrefaction in air and nitrogen. Energy & Fuels. 2014;28:3110-21. doi: 10.1021/ef4022202.
23. Wannapeera J, Worasuwannarak N. Upgrading of woody biomass by torrefaction under pressure. J Anal Appl Pyrolysis. 2012;96:173-80. doi: 10.1016/j.jaap.2012.04.002.
24. Setkit N, Li X, Yao H, Worasuwannarak N. Torrefaction behavior of hot-pressed pellets prepared from leucaena wood. Bioresour Technol. 2021;321:124502. doi: 10.1016/j.biortech.2020.124502.
25. Kaewtrakulchai N, Wisetsai A, Phongaksorn M, Thipydet C, Jongsomjit B, Laosiripojana N, et al. Parametric study on mechanical-press torrefaction of palm oil empty fruit bunch for production of biochar. Carb Resour Convers. 2025;8:100285. doi: 10.1016/j.crcon.2024.100285.
26. Setkit N, Li X, Yao H, Worasuwannarak N. Torrefaction under mechanical pressure of 10–70 MPa at 250 °C and its effect on pyrolysis behaviours of leucaena wood. Bioresour Technol. 2021;338:125503. doi: 10.1016/j.biortech.2021.125503.
27. Shi L, Hu Z, Li X, Li S, Yi L, Wang X, et al. Gas-pressurized torrefaction of lignocellulosic solid wastes: Low-temperature deoxygenation and chemical structure evolution mechanisms. Bioresour Technol. 2023;385:129414. doi: 10.1016/j.biortech.2023.129414.
28. Apaydın-Varol E, Pütün AE. Preparation and characterization of pyrolytic chars from different biomass samples. J Anal Appl Pyrolysis. 2012;98:29-36. doi: 10.1016/j.jaap.2012.07.001.
29. Channiwala SA, Parikh PP. A unified correlation for estimating HHV of solid, liquid and gaseous fuels. Fuel. 2002;81:1051-63. doi: 10.1016/S0016-2361(01)00131-4.
30. Libra JA, Ro KS, Kammann C, Funke A, Berge ND, Neubauer Y, et al. Hydrothermal carbonization of biomass residuals: A comparative review of the chemistry, processes and applications of wet and dry pyrolysis. Biofuels. 2011;2:71-106. doi: 10.4155/bfs.10.81.
31. Kaewtrakulchai N, Chanpee S, Jadsadajerm S, Wongrerkdee S, Manatura K, Eiad-Ua A. Co-hydrothermal carbonization of polystyrene waste and maize stover combined with KOH activation to develop nanoporous carbon as catalyst support for catalytic hydrotreating of palm oil. Carb Resour Convers. 2024;7:100231. doi: 10.1016/j.crcon.2024.100231.

32. Wannapeera J, Li X, Worasuwannarak N, Ashida R, Miura K. Production of high-grade carbonaceous materials and fuel having similar chemical and physical properties from various types of biomass by degradative solvent extraction. Energy & Fuels. 2012;26:4521-31. doi: 10.1021/ef3003153.
33. Jadsadajerm S, Muangthong-on T, Wannapeera J, Ohgaki H, Miura K, Worasuwannarak N. Degradative solvent extraction of biomass using petroleum based solvents. Bioresour Technol. 2018;260:169-76. doi: 10.1016/j.biortech.2018.03.124.
34. Sonobe T, Worasuwannarak N. Kinetic analyses of biomass pyrolysis using the distributed activation energy model. Fuel. 2008;87:414-21. doi: 10.1016/j.fuel.2007.05.004.
35. Antal MJ, Grønli M. The art, science, and technology of charcoal production. Ind Eng Chem Res. 2003;42:1619-40. doi: 10.1021/ie0207919.
36. Bridgwater A. Fast pyrolysis processes for biomass. Renew Sustain Energy Rev. 2000;4:1-73. doi: 10.1016/S1364-0321(99)00007-6.

How to cite this article:
Wannapeera J, Hinsui T, Jadsadajerm S, Liplap P. Upgrading bio-oil quality via pressurized air pretreatment of lignocellulosic biomass. J Sustain Res. 2025;7(4):e250066. https://doi.org/10.20900/jsr20250066.